Atmos. Chem. Phys. Discuss., 12, 28929–28953, 2012
www.atmos-chem-phys-discuss.net/12/28929/2012/
doi:10.5194/acpd-12-28929-2012

Atmospheric Chemistry and Physics Discussions

Black carbon vertical profiles strongly affect its radiative forcing uncertainty

B. H. Samset[1], G. Myhre[2], M. Schulz[1], Y. Balkanski[3], S. Bauer[4], T. K. Berntsen[1], H. Bian[5], N. Bellouin[6], T. Diehl[7,8], R. C. Easter[9], S. J. Ghan[9], T. Iversen[2,11], S. Kinne[10], A. Kirkevåg[2], J.-F. Lamarque[12], G. Lin[13], X. Liu[9], J. Penner[13], Ø. Seland[2], R.B. Skeie[1], P. Stier[14], T. Takemura[15], K. Tsigaridis[4], and K. Zhang[9,10]

[1]Center for International Climate and Environmental Research – Oslo (CICERO), Oslo, Norway
[2]Norwegian Meteorological Institute, Oslo, Norway
[3]Laboratoire des Sciences du Climat et de l'Environnement, CEA-CNRS-UVSQ, Gif-sur-Yvette, France
[4]NASA Goddard Institute for Space Studies and Columbia Earth Institute, New York, NY, USA
[5]Earth System Science Interdisciplinary Center, University of Maryland, College Park, MD, USA
[6]Met Office Hadley Centre, Exeter, UK
[7]NASA Goddard Space Flight Center, Greenbelt, MD, USA
[8]Universities Space Research Association, Columbia, MD, USA
[9]Pacific Northwest National Laboratory, Richland, WA, USA
[10]Max Planck Institute for Meteorology, Hamburg, Germany

[11]Department of Geosciences, University of Oslo, Oslo, Norway
[12]NCAR Earth System Laboratory, National Center for Atmospheric Research, Boulder, CO, USA
[13]Department of Atmospheric, Oceanic, and Space Sciences, University of Michigan, Ann Arbor, Michigan, USA
[14]University of Oxford, Oxford, UK
[15]Research Institute for Applied Mechanics, Kyushu University, Fukuoka, Japan

Received: 22 October 2012 – Accepted: 29 October 2012 – Published: 7 November 2012

Correspondence to: B. H. Samset (b.h.samset@cicero.uio.no)

Published by Copernicus Publications on behalf of the European Geosciences Union.

ACPD
12, 28929–28953, 2012

Abstract

The impact of black carbon (BC) aerosols on the global radiation balance is not well constrained. Here twelve global aerosol models are used to show that at least 20 % of the present uncertainty in modeled BC direct radiative forcing (RF) is due to diversity in the simulated vertical profile of BC mass. Results are from phases 1 and 2 of the global aerosol model intercomparison project (AeroCom). Additionally, a significant fraction of the variability is shown to come from high altitudes, as, globally, more than 40 % of the total BC RF is exerted above 5 km. BC emission regions and areas with transported BC are found to have differing characteristics. These insights into the importance of the vertical profile of BC lead us to suggest that observational studies are needed to better characterize the global distribution of BC, including in the upper troposphere.

1 Introduction

Unlike most atmospheric aerosols, black carbon (BC) absorbs solar radiation. This warming effect of BC has led to suggestions, both in the scientific community (Editorial, 2009; Grieshop et al., 2009; Hansen et al., 2000; Shindell et al., 2012) and among policy makers, for reduction of BC emissions to mitigate global warming. The uncertainties in the radiative forcing (RF) of the direct aerosol effect of BC are however large (Feichter and Stier, 2012; Ramanathan and Carmichael, 2008; Schulz et al., 2006), hampering mitigation studies (Koch et al., 2011a). Among the causes of these model uncertainties are assumptions about the vertical concentration profiles of BC (Zarzycki and Bond, 2010). There are also significant discrepancies between models and observations (Koch et al., 2009).

Aerosol radiative forcing is a measure of the effect a given change in aerosol concentrations has on the atmospheric energy balance. The efficiency with which BC can induce RF is however dependent on external factors such as surface albedo, water vapor, background aerosol distributions and, most notably, the presence of clouds (Haywood and Shine, 1997; Zarzycki and Bond, 2010). The BC forcing is therefore highly sensitive to the full 3-D distribution of BC concentration (Samset and Myhre, 2011). Anthropogenic direct BC forcing estimated by the current major global aerosol models varies between 0.05 $\mathrm{W\,m^{-2}}$ and 0.38 $\mathrm{W\,m^{-2}}$ (Myhre et al., 2012). This range is similar to earlier estimates (Feichter and Stier, 2012; Schulz et al., 2006), and difficulties in reducing the range highlights the urgent need to understand the different causes of this model variability in BC forcing.

Several studies have previously indicated that the vertical transport is one area where the models still differ significantly (Koffi et al., 2012; Schwarz et al., 2010; Textor et al., 2006, 2007). This study uses input from 12 global aerosol models participating in the AeroCom model intercomparison project to compare and study the impacts of modeled BC vertical forcing profiles. By combining the models' own concentration profiles with a common 4-D (spatial and temporal) efficiency profile (EP) of RF per gram of BC, we here recalculate and compare the exerted RF of the BC direct aerosol effect at various altitudes and spatial regions. By comparing calculations using the full 4-D in clear and cloudy skies with analyses using global and annual mean profiles, we can also isolate the contributions from the cloud field and variations due to regional differences.

2 Data

The AeroCom initiative asks models to simulate the direct aerosol radiative effect under as similar conditions as possible. All models run single year simulations using the same base years for aerosol emissions (2000 and 1850), with unchanged meteorology to exclude indirect effects. Both circulation models and transport models have participated. Two sets of model intercomparisons have been performed, here labeled AeroCom Phase 1 (Kinne et al., 2006; Schulz et al., 2006; Textor et al., 2006) and AeroCom Phase 2 (Myhre et al., 2012). See the references or the main AeroCom website (aerocom.met.no) for details.

Discussion Paper | Discussion Paper | Discussion Paper | Discussion Paper |
ACPD
12, 28929–28953, 2012

Black carbon vertical profiles strongly affect

B. H. Samset et al.

For the present study, 4-D (spatial and temporal) BC concentration fields from 12 global aerosol models participating in AeroCom Phase 2 are used. For six of the models, concentration fields of BC from fossil and biofuel burning only (BCFF) are also used. The 1850 concentrations are subtracted from the 2000 ones, leaving the contribution due to anthropogenic BC or BCFF emissions. Unless otherwise stated, all results below are for anthropogenic aerosols only.

Three of the same modeling groups also provided BC concentration profiles to AeroCom Phase 1, and these fields are also included here. The IMPACT model has not undergone major changes between the AeroCom phases, and for CAM4-Oslo the changes related to the treatment of BC are small. The OsloCTM2 model has however been heavily revised with the addition of both an ageing scheme for BC and improved treatment of BC washout between P1 and P2.

From AeroCom P2, participating models are NCAR-CAM3.5 (Lamarque et al., 2012), CAM4-Oslo (Kirkevåg et al., 2012), CAM5.1 (Liu et al., 2012), GISS-modelE (Koch et al., 2011b), GMI (Bian et al., 2009), GOCART-v4 (Chin et al., 2009), HadGEM2 (Bellouin et al., 2011), IMPACT (Lin et al., 2012), INCA (Szopa et al., 2012), ECHAM5-HAM (Zhang et al., 2012), OsloCTM2 (Skeie et al., 2011) and SPRINTARS (Takemura et al., 2005). From AeroCom P1, participating models are UiO_GCM (Kirkevag and Iversen, 2002) (earlier version of CAM4-Oslo), IMPACT (Liu et al., 2005) and OsloCTM2 (denoted as UiO_CTM in AeroCom P1) (Myhre et al., 2003).

3 Methods

3.1 4-dimensional forcing efficiency profiles

Samset and Myhre (2011) presented a set of vertical profiles of the direct radiative forcing per gram of aerosol for BCFF, i.e. the amount of top-of-atmosphere shortwave radiative forcing seen by a particular model (OsloCTM2) per gram of aerosols at a given altitude. Here we term these efficiency profiles (EP). In the literature, the term

Discussion Paper | Discussion Paper | Discussion Paper | Discussion Paper |

ACPD

12, 28929–28953, 2012

Black carbon vertical profiles strongly affect

B. H. Samset et al.

normalized radiative forcing is also commonly used. We here employ the full 4-D efficiency profiles, either for all sky or clear sky conditions. For each model grid point and time step, we multiply the modeled BC concentration by the EP to get the contribution to the total shortwave, top-of-atmosphere BC radiative forcing. This gives us intercomparable 4-D RF fields, something that is not immediately available from each model.

Differences in model specific treatment of clouds, water uptake and microphysics are removed by this method, and we are left solely with variations due to the concentration profiles and the total aerosol burden. We label this the recalculated RF, to emphasize that it is heavily correlated with the burden and should not be taken directly as an estimate of BC forcing of each model. Since the model that was used to produce the profiles of RF per gram has among the strongest global mean forcing efficiencies (Myhre et al., 2012), most recalculated RFs can be expected to be stronger than their host model would predict. However, by dividing the recalculated RF by the total aerosol burden of the host model, we extract the variability in forcing per gram from each model that is due only to vertical profiles, and can subsequently use the vertical RF profiles to study it (see Sect. 4.1).

The remaining variability in forcing per gram contains information on regional differences (high or low surface albedo, indigenous emissions, transport region or both), and the impact of cloud fields. To study these effects, we ran parallel analyses using only a global mean profile of RF per gram (labeled GP above), a distinct profile of RF per gram for clear sky conditions (labeled CS), or both (labeled CSGP).

3.2 Region definitions

A set of illustrative regions is chosen for some of the results and discussion below. “Europe” is defined as the box covering longitudes −10 to 30, latitudes 38 to 60. “China” covers longitudes 105 to 135, latitudes 15 to 45. “Arctic” covers latitudes 70 to 90, all longitudes. Europe and China represent regions with high industrial BC emissions and significant fractions of the global BCFF emissions, making their total BC forcing

ACPD
12, 28929–28953, 2012

sensitive to pure vertical transport and wet scavenging. The Arctic is a region with low indigenous emissions, but important BC contributions at high altitudes transported from other regions. Its total BC forcing is therefore sensitive to model differences in vertical and long range transport.

4 Results

4.1 RF variability due to vertical profiles

We first quantify the fraction of the total modeled RF variability attributable to vertical profiles alone. Figure 1a shows the global mean anthropogenic BC burden from models participating in AeroCom Phase 2, in addition to three models from AeroCom Phase 1 included to investigate the magnitude of variability due to model developments. We find a multi-model mean of 0.19 mg m^{-2}, but with a relative standard deviation (RSD) of 32 % and a model spread from 0.09 to 0.37 mg m^{-2}. Table 1 lists the numbers for individual models. Under an assumption of equal forcing per gram, this alone will cause a large diversity in the total BC forcing predicted by the models. AeroCom Phases 1 and 2 found a similar burden range, as shown by the whisker boxes in Fig. 1a. Note that the AeroCom P1 includes BC from all sources, while P2 results are for BC from fossil and biofuel burning (BCFF) sources only. This causes the P2 burden and RF means to be lower than for P1 (see Discussion for further comments). Figure 1b shows the RF for each model, recalculated from the concentration profiles using a common EP (Samset and Myhre, 2011). These recalculated RF values are highly correlated (Pearson corr. coeff. $\rho = 95\,\%$) with the burden values. However, dividing the recalculated RF by the global mean burdens gives global estimates of BC forcing efficiency (radiative forcing exerted per gram of BC aerosol), that are independent of the burden value simulated by the host model. This is shown in Fig. 1c. If the modeled spatial and temporal aerosol distributions, notably the vertical profiles, were also identical this spread would vanish. The remaining diversity therefore carries information on the impact of the 4-D

BC concentration profiles on the model RF spread, separate from the variability due to burden differences.

To quantify this impact, we further analyze the multi-model RSDs and correlations. There is a residual variability in the forcing efficiency that is due to the variations in the 4-D (spatial and temporal) aerosol mass distributions, with a relative standard deviation (RSD) of 16 %. This number is dominated by the vertical distributions, but will also have components from horizontal and temporal variability between models. To isolate the contribution from vertical distributions, we performed the analysis using global mean BC and efficiency profiles per month, averaging out any horizontal differences, and then using global, annual mean profiles, to also remove temporal variability. The resulting RSD from vertical profiles alone is 13 %. This is approximately 30 % of the variability on forcing per burden in AeroCom P1 and P2. Three models in P2 have mass extinction coefficients that deviate significantly from recommendations given in the literature (Bond et al., 2006). Removing contributions from these three models reduces the RSD on the forcing per burden to 32 %, subsequently increasing the estimate of the variability due to vertical profiles to 40 %.

The burden and forcing efficiencies in P1 and P2 have approximately equal RSDs, so if they were uncorrelated the vertical distribution could be said to contribute 20 % of the variability on RF. This is however not the case. We first note that in both AeroCom P1 and P2, the burdens and forcing efficiencies are weakly anticorrelated. This is apparent from the fact that the RSD on the RF (shown in Fig. 1) is lower than it would be if the errors on burden and forcing per burden were uncorrelated. Quantifying this effect using numbers from AeroCom P2, we find a weak Pearson correlation coefficient of $\rho = -0.46$ (or -0.40 if we again remove the three outlier models).

In the present analysis, we can estimate the impact of the vertical distributions by the fraction of mass simulated above 5 km (M5k), shown in Table 1. We observe that M5k is strongly correlated with the recalculated RF ($\rho = 0.70$) and forcing per burden ($\rho = 0.97$), as expected due to the efficiency profile used for the present analysis. However M5k is also weakly positively correlated with the total burden ($\rho = 0.48$). The

ACPD
12, 28929–28953, 2012

vertical distribution variability therefore does not contribute to the observed anticorrelation between burden and forcing per burden in AeroComP1 and P2.

We can assume that forcing per burden is determined by a combination of the vertical profile (positive correlation with burden) and a set of uncorrelated global variables such as BC optical properties (which must then have a combined negative correlation with burden). The variability on BC RF would be higher if the models had not compensated for high burden with a low forcing efficiency and vice versa. Since the vertical variability rather leads to a high efficiency for a high burden, its impact on the RF variability is likely stronger than the minimum estimate of 20 % above. The present analysis does not allow for rigorous quantification, but it is unlikely to be larger than the 50 % of the variability on total BC RF caused by forcing per burden. Hence we have a range of 20 % to 50 % of the variability of modeled BC RF caused by differences in vertical distributions.

4.2 Comparison of modeled RF profiles

Next we compare global and regional BC vertical profiles and EPs. As also shown in previous model comparisons (Schwarz et al., 2010; Textor et al., 2006, 2007), there are large differences in the modeled BC concentrations. Figure 2a–c shows the annual mean vertical profiles of BC concentration from all models, globally and for two selected regions (Arctic and China). Globally, the concentrations quickly decrease with altitude while the forcing efficiency increases. The Arctic is a region with negligible indigenous BC emissions, but where the effects of transported aerosols are relevant (Shindell et al., 2008). While all models show a significant BC contribution at high altitudes the model spread in the Arctic is significant, ranging from virtually constant below 200 hPa to double-peaked structures with maxima at 900 hPa and 200 hPa. This highlights the differences in transport and wet removal schemes between the climate models. AeroCom P1 and P2 models can be seen to perform similarly where we are able to compare. China has large surface emissions of BC, and also sees contributions from transport at high altitudes, as is evident from Fig. 2c.

ACPD
12, 28929–28953, 2012

Figure 2d–f shows the corresponding recalculated forcing efficiency as a function of altitude, divided by model layer height to remove differences due to the models' vertical resolution. The resulting vertical profiles illustrate at what altitudes RF is exerted. Globally, RF can be seen to be mostly exerted in a range around 800 hPa for most models, with a secondary peak between 400 hPa and 200 hPa for some models. The China region follows the global pattern, but with the low altitude peak closer to the ground, reflecting the emissions there. The Arctic region, however, has a strong peak at high altitudes for most models, evidencing the relative importance of high altitude BC RF there. These features are explainable by the differences in regional concentration and forcing efficiency profiles shown in Fig. 2a–c.

Figure 2g–i illustrates the model spread in accumulated forcing, by integrating the absolute forcing per model layer from the surface and upwards. Globally, several of the models exert 50 % of their forcing above 5 km; however there is a large spread around this value. Regionally, this picture is quite different. In the Arctic all models have a significant forcing component above 5 km, due both to a high fraction of aerosol at high altitudes and a strong forcing efficiency caused by high surface albedo. For the industrial regions of China the opposite is true, with the bulk of the aerosol located close to the ground where the forcing efficiency is weak.

4.3 RF fraction exerted at high altitudes

We find, in general, that a significant fraction of modeled BC RF is exerted at high altitudes, with a notable regional pattern. Figure 3 maps the model mean fraction of aerosol mass (3a) and induced forcing (3b) from model layers of altitude above 500 hPa, or approximately 5 km. Firstly, the distinction between BC emission regions and regions with mostly transported BC is evident. The former have small mass and RF fractions at high altitudes, typically 10–20 %, while transport regions show RF fractions up to 80 %. Figure 3c compares the global and regional (Arctic, China and Europe) mean values of the mass and RF fractions. Note that the fraction of RF above 5 km is systematically higher than the mass fraction, due to the strongly increasing shape of

Discussion Paper | Discussion Paper | Discussion Paper | Discussion Paper |

ACPD

12, 28929–28953, 2012

Black carbon vertical profiles strongly affect

B. H. Samset et al.

the RF efficiency profiles. Globally, more than 40 % of the model simulated RF from BC comes from model layers above 5 km, while only 24 % of the mass is found in this region. This illustrates the importance of validating model vertical profiles and transport codes not only in industrial regions, but also in transport regions with low indigenous BC emissions.

Figure 4 shows the RF and mass fractions in four altitude bands, globally and for the three regions. Selected bands are 0–2 km, 2–5 km, 5–10 km and above 10 km. Altitudes are chosen by finding the model layer with a global mean pressure that closest approximates the desired height. Such information is useful for comparing models with observational data, which are typically given for given altitude bands. This can in turn aid future constructions of best estimates for global BC forcing. We note that the pattern of high variability between model estimates of burden and forcing is apparent in all four bands chosen.

4.4 Variability in forcing efficiency due to clouds and regional differences

We have shown that, even on global mean, a significant fraction of the variability in the BC forcing per gram is due to differences in vertical profiles. It is instructive to further divide this variability into the components that make up the efficiency profiles. In Fig. 5a we show the zonal mean forcing efficiency for all models, and investigate the relative importance of the cloud field and of regional differences in albedo for the resulting spread. In Fig. 5c we have run the analysis using a global, annual mean efficiency profile instead of the full 4-D profile, and in addition used clear sky conditions. The forcing efficiency has a weak but non-vanishing model spread, and is only weakly dependent on latitude since the effects of varying surface albedo, which normally strongly increases the forcing efficiency at the poles, are averaged out in the global profile. Not all vertical sensitivity of BC forcing is due to the aerosols being above or below clouds (Samset and Myhre, 2011). The remainder, caused predominantly by Rayleigh scattering, water vapor and the competing effects of other aerosols, is the cause of the variability here. RSD on global mean values is 10 % (see Fig. 5b). Figure 5d shows the same analysis using the full 3-D efficiency profile. The RSD increases to 13 %, and we now see the latitudinal effects of the high polar planetary albedo. Figure 4e shows the analysis using the global mean efficiency profile again, but under all-sky conditions. Again the RSD increases to 13 %, due to the cloud field. The model variability in forcing efficiency that is due to vertical profile differences can therefore be decomposed into three factors: Equal and significant contributions from the cloud field and from regional differences, and a major contribution from the underlying sensitivity of BC forcing to altitude even in the absence of clouds and albedo differences. Harmonizing model treatment of clouds and albedo is therefore not sufficient to remove uncertainties in BC forcing due to vertical profiles, highlighting the importance of ongoing aerosol model intercomparisons emphasizing other sources of variability (Stier, 2012). Combining the effects of clouds and regional variations with the intrinsic vertical variability of the forcing efficiency yields the total variability picture seen in Fig. 5a.

5 Discussions

The model mean direct BC forcing recalculated above is stronger than in previous estimates (Feichter and Stier, 2012; Schulz et al., 2006). This is mainly due to the fact that the host model for the efficiency profiles, OsloCTM2, has a high mean forcing efficiency compared to the others (Myhre et al., 2012). The RF numbers in the present paper should therefore not be taken as new estimates for absolute direct RF forcing. We also observe that the recalculated RF values are highly correlated (95 %) with modeled burden values. This is again expected, and is due to the use of a common BC EP.

Different models will likely have different BC efficiency profiles. To quantify the sensitivity of the present analysis to the shape of the profile used, we reran the analysis with an EP that was changed by 20 % at the top of the atmosphere and unchanged at the surface, with a linear interpolation in between, resulting in a weaker EP. This changed the global fraction of RF above 5km by less than 5 %, indicating that the results are relatively stable within reasonable variations of the EP.

Discussion Paper | Discussion Paper | Discussion Paper | Discussion Paper |

ACPD

12, 28929–28953, 2012

Results in the present study are given for total BC aerosol emissions only. However, due to different source regions, the vertical profiles of BCFF could be different from BC. Six models also provided concentration profiles for BCFF. Using the same efficiency profiles we performed the analysis also for BCFF, and found results consistent with what we have presented for BC (not shown). While the absolute forcing numbers differ due to lower total burdens for BCFF, the variability in vertical profiles is very similar to that for total BC. Our conclusions here are therefore also applicable to model comparison results on BCFF only.

Results presented here have all used emissions from year 2000. One model (CAM4-Oslo) also provided simulations for year 2006. While the BC burden was 60 % higher for 2006 emissions, the forcing efficiencies and vertical profiles were invariant. This gives confidence that the variability due to vertical profiles can indeed be regarded as independent of that due to the present day emissions dataset.

Results for the P1 and P2 submissions of the IMPACT model, where no major aerosol microphysical changes have been performed, are quite similar. For OsloCTM2, however, where both an ageing scheme and modifications to the washout of BC were added, the forcing efficiency changes between P1 and P2 by as much as half of the full range observed. Hence, the transport scheme and model treatment of BC are crucial factors in determining the modeled value of forcing efficiency, and both of these factors are closely linked to the vertical distribution.

6 Conclusions

We have shown that the previously documented large spread in BC aerosol concentration profiles is enhanced for vertical BC RF profiles. Using 12 global aerosol models, we show that most models globally exert 40 % of their BC forcing above 5 km, and that regionally the fraction can be above 70 %. The spread between models is however quite large, and we computed that at least 20 %, possibly as much as 50 %, of the differences in modeled BC RF can be attributed to differences in vertical profiles.

ACPD
12, 28929–28953, 2012

Harmonizing the treatment of clouds and albedo between models is found to not be sufficient to remove this variability. To propose efficient mitigation measures for BC, its radiative forcing needs to be well understood both in emission and transport regions. Further model improvements and comparisons with data are needed, and should focus on both of these types of region. Observational studies are needed to provide input to modelers, with the aim of better characterizing the global distribution of BC, especially in the upper troposphere. It is however clear that while the BC vertical profiles are important, they are not sufficient to explain all the remaining differences between global aerosol models. Further model intercomparison studies, e.g. on BC optical properties, surface albedo, treatment of clouds and aerosol transport and washout, are therefore also needed if the impact of BC on the global radiation balance is to be sufficiently constrained.

Acknowledgements. S. Ghan, X. Liu and R. Easter were funded by the US Department of Energy, Office of Science, Scientific Discovery through Advanced Computing (SciDAC) Program and by the Office of Science Earth System Modeling Program. Computing resources were provided by the Climate Simulation Laboratory at NCAR's Computational and Information Systems Laboratory (CISL), sponsored by the National Science Foundation and other agencies. The Pacific Northwest National Laboratory is operated for DOE by Battelle Memorial Institute under contract DE-AC06-76RLO 1830. Simulations of the ECHAM5-HAM, INCA, CAM4-Oslo and HadGEM2 models have been supported with funds from the FP6 project EUCAARI (Contract 34684). A. Kirkevag, T. Iversen and Ø. Seland (CAM4-Oslo) were supported by the Research Council of Norway through the EarthClim (207711/E10) and NOTUR/NorStore projects, by the Norwegian Space Centre through PM-VRAE, and through the EU projects PEGASOS and ACCESS. G. Myhre and B. Samset were funded by the Research Council of Norway through the EarthClim and SLAC projects.

ACPD
12, 28929–28953, 2012

References

Bellouin, N., Rae, J., Jones, A., Johnson, C., Haywood, J., and Boucher, O.: Aerosol forcing in the Climate Model Intercomparison Project (CMIP5) simulations by HadGEM2-ES and the role of ammonium nitrate, J. Geophys. Res.-Atmos., 116, D20206, doi:10.1029/2011jd016074, 2011.

Bian, H., Chin, M., Rodriguez, J. M., Yu, H., Penner, J. E., and Strahan, S.: Sensitivity of aerosol optical thickness and aerosol direct radiative effect to relative humidity, Atmos. Chem. Phys., 9, 2375–2386, doi:10.5194/acp-9-2375-2009, 2009.

Bond, T. C., Habib, G., and Bergstrom, R. W.: Limitations in the enhancement of visible light absorption due to mixing state, J. Geophys. Res.-Atmos., 111, D20211, doi:10.1029/2006jd007315, 2006.

Chin, M., Diehl, T., Dubovik, O., Eck, T. F., Holben, B. N., Sinyuk, A., and Streets, D. G.: Light absorption by pollution, dust, and biomass burning aerosols: a global model study and evaluation with AERONET measurements, Ann. Geophys., 27, 3439–3464, doi:10.5194/angeo-27-3439-2009, 2009.

Editorial, N.: Time for early action, Nature, 460, 12–12, 2009.

Feichter, J. and Stier, P.: Assessment of black carbon radiative effects in climate models, Wiley Interdisciplinary Reviews-Climate Change, 3, 359–370, doi:10.1002/Wcc.180, 2012.

Grieshop, A. P., Reynolds, C. C. O., Kandlikar, M., and Dowlatabadi, H.: A black-carbon mitigation wedge, Nature Geoscience, 2, 533–534, 2009.

Hansen, J., Sato, M., Ruedy, R., Lacis, A., and Oinas, V.: Global warming in the twenty–first century: An alternative scenario, P. Natl. Acad. Sci. USA, 97, 9875–9880, 2000.

Haywood, J. M. and Shine, K. P.: Multi-spectral calculations of the direct radiative forcing of tropospheric sulphate and soot aerosols using a column model, Q. J. Roy. Meteor. Soc., 123, 1907–1930, 1997.

Dentener, F., Kinne, S., Bond, T., Boucher, O., Cofala, J., Generoso, S., Ginoux, P., Gong, S., Hoelzemann, J. J., Ito, A., Marelli, L., Penner, J. E., Putaud, J.-P., Textor, C., Schulz, M., van der Werf, G. R., and Wilson, J.: Emissions of primary aerosol and precursor gases in the years 2000 and 1750 prescribed data-sets for AeroCom, Atmos. Chem. Phys., 6, 4321–4344, doi:10.5194/acp-6-4321-2006, 2006.

Kirkevåg, A. and Iversen, T.: Global direct radiative forcing by process-parameterized aerosol optical properties, J. Geophys. Res.-Atmos., 107, 4433, doi:10.1029/2001jd000886, 2002.

Kirkevåg, A., Iversen, T., Seland, Ø., Hoose, C., Kristjáson, J. E., Struthers, H., Ekman, A., Ghan, S., Griesfeller, J., Nilsson, D., and Schulz, M.: Aerosol-climate interactions in the Norwegian Earth System model – Nor ESM, Geosci. Model Dev. Discuss., in preparation, 2012.
Koch, D., Schulz, M., Kinne, S., McNaughton, C., Spackman, J. R., Balkanski, Y., Bauer, S., Berntsen, T., Bond, T. C., Boucher, O., Chin, M., Clarke, A., De Luca, N., Dentener, F., Diehl, T., Dubovik, O., Easter, R., Fahey, D. W., Feichter, J., Fillmore, D., Freitag, S., Ghan, S., Ginoux, P., Gong, S., Horowitz, L., Iversen, T., Kirkevåg, A., Klimont, Z., Kondo, Y., Krol, M., Liu, X., Miller, R., Montanaro, V., Moteki, N., Myhre, G., Penner, J. E., Perlwitz, J., Pitari, G., Reddy, S., Sahu, L., Sakamoto, H., Schuster, G., Schwarz, J. P., Seland, Ø., Stier, P., Takegawa, N., Takemura, T., Textor, C., van Aardenne, J. A., and Zhao, Y.: Evaluation of black carbon estimations in global aerosol models, Atmos. Chem. Phys., 9, 9001–9026, doi:10.5194/acp-9-9001-2009, 2009.
Koch, D., Balkanski, Y., Bauer, S. E., Easter, R. C., Ferrachat, S., Ghan, S. J., Hoose, C., Iversen, T., Kirkev
ag, A., Kristjansson, J. E., Liu, X., Lohmann, U., Menon, S., Quaas, J., Schulz, M., Seland, Ø., Takemura, T., and Yan, N.: Soot microphysical effects on liquid clouds, a multi-model investigation, Atmos. Chem. Phys., 11, 1051–1064, doi:10.5194/acp-11-1051-2011, 2011a.
Koch, D., Bauer, S. E., Del Genio, A., Faluvegi, G., McConnell, J. R., Menon, S., Miller, R. L., Rind, D., Ruedy, R., Schmidt, G. A., and Shindell, D.: Coupled Aerosol-Chemistry-Climate Twentieth-Century Transient Model Investigation: Trends in Short-Lived Species and Climate Responses, J. Climate, 24, 2693–2714, 2011b.
Koffi, B., Schulz, M., Breon, F. M., Griesfeller, J., Winker, D., Balkanski, Y., Bauer, S., Berntsen, T., Chin, M. A., Collins, W. D., Dentener, F., Diehl, T., Easter, R., Ghan, S., Ginoux, P., Gong, S. L., Horowitz, L. W., Iversen, T., Kirkevag, A., Koch, D., Krol, M., Myhre, G., Stier, P., and Takemura, T.: Application of the CALIOP layer product to evaluate the vertical distribution of aerosols estimated by global models: AeroCom phase I results, J. Geophys. Res.-Atmos., 117, D10201, doi:10.1029/2011jd016858, 2012.
Lamarque, J.-F., Emmons, L. K., Hess, P. G., Kinnison, D. E., Tilmes, S., Vitt, F., Heald, C. L., Holland, E. A., Lauritzen, P. H., Neu, J., Orlando, J. J., Rasch, P. J., and Tyndall, G. K.: CAM-chem: description and evaluation of interactive atmospheric chemistry in the Community Earth System Model, Geosci. Model Dev., 5, 369–411, doi:10.5194/gmd-5-369-2012, 2012.

ACPD
12, 28929–28953, 2012

Black carbon vertical profiles strongly affect

B. H. Samset et al.

Lin, G., Penner, J. E., Sillman, S., Taraborrelli, D., and Lelieveld, J.: Global modeling of SOA formation from dicarbonyls, epoxides, organic nitrates and peroxides, Atmos. Chem. Phys., 12, 4743–4774, doi:10.5194/acp-12-4743-2012, 2012.

Liu, X. H., Penner, J. E., and Herzog, M.: Global modeling of aerosol dynamics: Model description, evaluation, and interactions between sulfate and nonsulfate aerosols, J. Geophys. Res.-Atmos., 110, D18206, doi:10.1029/2004jd005674, 2005.

Liu, X., Easter, R. C., Ghan, S. J., Zaveri, R., Rasch, P., Shi, X., Lamarque, J.-F., Gettelman, A., Morrison, H., Vitt, F., Conley, A., Park, S., Neale, R., Hannay, C., Ekman, A. M. L., Hess, P., Mahowald, N., Collins, W., Iacono, M. J., Bretherton, C. S., Flanner, M. G., and Mitchell, D.: Toward a minimal representation of aerosols in climate models: description and evaluation in the Community Atmosphere Model CAM5, Geosci. Model Dev., 5, 709–739, doi:10.5194/gmd-5-709-2012, 2012.

Myhre, G., Berntsen, T. K., Haywood, J. M., Sundet, J. K., Holben, B. N., Johnsrud, M., and Stordal, F.: Modeling the solar radiative impact of aerosols from biomass burning during the Southern African Regional Science Initiative (SAFARI-2000) experiment, J. Geophys. Res.-Atmos., 108, 8501, doi:10.1029/2002jd002313, 2003.

Myhre, G., Samset, B. H., Schulz, M., Balkanski, Y., Bauer, S., Berntsen, T. K., Bian, H., Bellouin, N., Chin, M., Diehl, T., Easter, R. C., Feichter, J., Ghan, S. J., Hauglustaine, D., Iversen, T., Kinne, S., Kirkevåg, A., Lamarque, J.-F., Lin, G., Liu, X., Luo, G., Ma, X., Penner, J. E., Rasch, P. J., Seland, Ø., Skeie, R. B., Stier, P., Takemura, T., Tsigaridis, K., Wang, Z., Xu, L., Yu, H., Yu, F., Yoon, J.-H., Zhang, K., Zhang, H., and Zhou, C.: Radiative forcing of the direct aerosol effect from AeroCom Phase II simulations, Atmos. Chem. Phys. Discuss., 12, 22355–22413, doi:10.5194/acpd-12-22355-2012, 2012.

Ramanathan, V. and Carmichael, G.: Global and regional climate changes due to black carbon, Nat. Geosci., 1, 221–227, 2008.

Samset, B. H. and Myhre, G.: Vertical dependence of black carbon, sulphate and biomass burning aerosol radiative forcing, Geophys. Res. Lett., 38, L24802, doi:10.1029/2011gl049697, 2011.

Schulz, M., Textor, C., Kinne, S., Balkanski, Y., Bauer, S., Berntsen, T., Berglen, T., Boucher, O., Dentener, F., Guibert, S., Isaksen, I. S. A., Iversen, T., Koch, D., Kirkevåg, A., Liu, X., Montanaro, V., Myhre, G., Penner, J. E., Pitari, G., Reddy, S., Seland, Ø., Stier, P., and Takemura, T.: Radiative forcing by aerosols as derived from the AeroCom present-day and pre-industrial simulations, Atmos. Chem. Phys., 6, 5225–5246, doi:10.5194/acp-6-5225-2006, 2006.

ACPD
12, 28929–28953, 2012

Schwarz, J. P., Spackman, J. R., Gao, R. S., Watts, L. A., Stier, P., Schulz, M., Davis, S. M., Wofsy, S. C., and Fahey, D. W.: Global scale black carbon profiles observed in the remote atmosphere and compared to models, Geophys. Res. Lett., 37, L18812, doi:10.1029/2010GL044372, 2010.

Shindell, D. T., Chin, M., Dentener, F., Doherty, R. M., Faluvegi, G., Fiore, A. M., Hess, P., Koch, D. M., MacKenzie, I. A., Sanderson, M. G., Schultz, M. G., Schulz, M., Stevenson, D. S., Teich, H., Textor, C., Wild, O., Bergmann, D. J., Bey, I., Bian, H., Cuvelier, C., Duncan, B. N., Folberth, G., Horowitz, L. W., Jonson, J., Kaminski, J. W., Marmer, E., Park, R., Pringle, K. J., Schroeder, S., Szopa, S., Takemura, T., Zeng, G., Keating, T. J., and Zuber, A.: A multi-model assessment of pollution transport to the Arctic, Atmos. Chem. Phys., 8, 5353–5372, doi:10.5194/acp-8-5353-2008, 2008.

Shindell, D., Kuylenstierna, J. C. I., Vignati, E., van Dingenen, R., Amann, M., Klimont, Z., Anenberg, S. C., Muller, N., Janssens-Maenhout, G., Raes, F., Schwartz, J., Faluvegi, G., Pozzoli, L., Kupiainen, K., Hoglund-Isaksson, L., Emberson, L., Streets, D., Ramanathan, V., Hicks, K., Oanh, N. T. K., Milly, G., Williams, M., Demkine, V., and Fowler, D.: Simultaneously Mitigating Near-Term Climate Change and Improving Human Health and Food Security, Science, 335, 183–189, 2012.

Skeie, R. B., Berntsen, T., Myhre, G., Pedersen, C. A., Ström, J., Gerland, S., and Ogren, J. A.: Black carbon in the atmosphere and snow, from pre-industrial times until present, Atmos. Chem. Phys., 11, 6809–6836, doi:10.5194/acp-11-6809-2011, 2011.

Stier, P., Schutgens, N. A. J., Bian, H., Boucher, O., Chin, M., Ghan, S., Huneeus, N., Kinne, S., Lin, G., Myhre, G., Penner, J. E., Randles, C., Samset, B., Schulz, M., Yu, H., and Zhou, C.: Host model uncertainties in aerosol radiative forcing estimates: results from the AeroCom prescribed intercomparison study, Atmos. Chem. Phys. Discuss., 12, 25487–25549, doi:10.5194/acpd-12-25487-2012, 2012.

Szopa, S., Balkanski, Y., Schulz, M., Bekki, S., Cugnet, D., Fortems–Cheiney, A., Turquety, S., Cozic, A., Deandreis, C., Hauglustaine, D., Idelkadi, A., Lathiere, J., Marchand, M., Yan, N. and Dufresne, J.-L.: Aerosol and ozone changes as forcing for climate evolution between 1850 and 2100, Clim. Dynam., doi:10.1007/s00382-012-1408-y, in press, 2012.

Takemura, T., Nozawa, T., Emori, S., Nakajima, T. Y., and Nakajima, T.: Simulation of climate response to aerosol direct and indirect effects with aerosol transport-radiation model, J. Geophys. Res.-Atmos., 110, D02202, doi:10.1029/2004jd005029, 2005.

Textor, C., Schulz, M., Guibert, S., Kinne, S., Balkanski, Y., Bauer, S., Berntsen, T., Berglen, T., Boucher, O., Chin, M., Dentener, F., Diehl, T., Easter, R., Feichter, H., Fillmore, D., Ghan, S., Ginoux, P., Gong, S., Grini, A., Hendricks, J., Horowitz, L., Huang, P., Isaksen, I., Iversen, I., Kloster, S., Koch, D., Kirkevåg, A., Kristjansson, J. E., Krol, M., Lauer, A., Lamarque, J. F., Liu, X., Montanaro, V., Myhre, G., Penner, J., Pitari, G., Reddy, S., Seland, Ø., Stier, P., Takemura, T., and Tie, X.: Analysis and quantification of the diversities of aerosol life cycles within AeroCom, Atmos. Chem. Phys., 6, 1777–1813, doi:10.5194/acp-6-1777-2006, 2006.

Textor, C., Schulz, M., Guibert, S., Kinne, S., Balkanski, Y., Bauer, S., Berntsen, T., Berglen, T., Boucher, O., Chin, M., Dentener, F., Diehl, T., Feichter, J., Fillmore, D., Ginoux, P., Gong, S., Grini, A., Hendricks, J., Horowitz, L., Huang, P., Isaksen, I. S. A., Iversen, T., Kloster, S., Koch, D., Kirkevåg, A., Kristjansson, J. E., Krol, M., Lauer, A., Lamarque, J. F., Liu, X., Montanaro, V., Myhre, G., Penner, J. E., Pitari, G., Reddy, M. S., Seland, Ø., Stier, P., Takemura, T., and Tie, X.: The effect of harmonized emissions on aerosol properties in global models – an AeroCom experiment, Atmos. Chem. Phys., 7, 4489–4501, doi:10.5194/acp-7-4489-2007, 2007.

Zarzycki, C. M. and Bond, T. C.: How much can the vertical distribution of black carbon affect its global direct radiative forcing?, Geophys. Res. Lett., 37, L20807, doi:10.1029/2010gl044555, 2010.

Zhang, K., O'Donnell, D., Kazil, J., Stier, P., Kinne, S., Lohmann, U., Ferrachat, S., Croft, B., Quaas, J., Wan, H., Rast, S., and Feichter, J.: The global aerosol–climate model ECHAM-HAM, version 2: sensitivity to improvements in process representations, Atmos. Chem. Phys., 12, 8911–8949, doi:10.5194/acp-12-8911-2012, 2012.

Table 1. Modeled BC burden, RF calculated by use of full 4-D efficiency profiles (RF), and forcing per gram (NRF). All numbers shown for global mean and for three selected regions. RF_fraction shows the fraction of the total BC forcing simulated within the stated region. Mass > 5 km and RF > 5 km show the fractions of aerosol mass and RF, respectively, simulated above an altitude of ∼ 5 km (500 hPa).

Model	Burden [mg m^{-2}]	RF [Wm^{-2}]	NRF [W g^{-1}]	RF fraction [%]	Mass > 5 km [%]	RF > 5 km [%]	Model	Burden [mg m^{-2}]	RF [Wm^{-2}]	NRF [W g^{-1}]	RF fraction [%]	Mass > 5 km [%]	RF > 5 km [%]
Global							Arctic						
CAM3.5	0.14	0.25	1801	100	20.3	39.3	CAM3.5	0.05	0.20	3907	2.5	63.2	76.1
CAM4-Oslo	0.22	0.54	2445	100	46.0	64.7	CAM4-Oslo	0.20	0.79	3877	4.4	60.9	71.0
CAM5.1	0.09	0.16	1655	100	18.1	36.4	CAM5.1	0.02	0.07	4187	1.4	81.6	88.5
GISS-modelE	0.21	0.40	1905	100	30.1	56.4	GISS-modelE	0.16	0.64	3889	4.7	65.7	77.2
GMI	0.16	0.25	1564	100	12.7	27.1	GMI	0.08	0.27	3584	3.3	44.5	54.5
GOCART	0.19	0.38	1982	100	27.1	46.3	GOCART	0.14	0.52	3746	4.1	53.2	64.1
HadGEM2	0.37	0.81	2185	100	33.6	50.6	HadGEM2	0.34	1.19	3465	4.4	40.3	52.1
IMPACT	0.17	0.24	1450	100	5.8	13.1	IMPACT	0.05	0.16	3214	1.9	35.9	48.1
INCA	0.23	0.41	1833	100	28.9	53.8	INCA	0.07	0.29	4016	2.1	78.8	89.2
MPIHAM	0.18	0.26	1492	100	10.8	25.7	MPIHAM	0.03	0.11	4078	1.2	75.5	89.2
OsloCTM2	0.20	0.40	2003	100	30.1	48.3	OsloCTM2	0.07	0.27	3879	2.0	71.0	82.4
SPRINTARS	0.19	0.37	1959	100	30.3	54.2	SPRINTARS	0.08	0.34	4413	2.8	83.1	89.9
CAM4-Oslo-P1	0.17	0.34	1955	100	26.4	46.9	CAM4-Oslo-P1	0.12	0.46	3716	4.1	48.9	61.1
IMPACT-P1	0.19	0.30	1546	100	14.2	30.7	IMPACT-P1	0.11	0.35	3266	3.5	39.4	52.9
OsloCTM2-P1	0.19	0.27	1477	100	11.7	24.2	OsloCTM2-P1	0.02	0.07	3637	0.7	63.0	80.4
Mean	0.19	0.36	1817	100	23.1	41.2	Mean	0.10	0.38	3792	2.9	60.3	71.8
Std.dev	0.06	0.16	288	0	10.8	14.5	Std.dev	0.09	0.30	328	1.3	16.0	15.2
Europe							China						
CAM3.5	0.20	0.27	1386	1.2	16.2	40.8	CAM3.5	0.89	1.17	1312	8.9	9.7	25.0
CAM4-Oslo	0.36	0.73	2029	1.4	36.2	60.1	CAM4-Oslo	0.84	1.35	1612	4.7	22.7	48.3
CAM5.1	0.21	0.25	1230	1.7	9.1	25.0	CAM5.1	0.65	0.74	1139	8.9	8.1	24.4
GISS-modelE	0.62	0.79	1276	2.0	16.5	43.6	GISS-modelE	1.60	1.89	1185	8.8	10.4	30.5
GMI	0.34	0.42	1229	1.8	7.8	20.4	GMI	1.29	1.42	1099	10.7	4.7	14.1
GOCART	0.30	0.48	1626	1.3	21.6	44.0	GOCART	1.12	1.50	1340	7.5	11.3	28.4
HadGEM2	0.58	1.09	1864	1.4	27.3	47.4	HadGEM2	2.08	3.29	1581	7.6	15.9	34.2
IMPACT	0.36	0.37	1036	1.6	4.3	13.0	IMPACT	0.83	0.94	1138	7.3	3.3	9.2
INCA	0.45	0.54	1206	1.4	17.4	49.6	INCA	1.06	1.27	1198	5.7	13.7	40.8
MPIHAM	0.39	0.41	1052	1.6	5.8	19.4	MPIHAM	1.31	1.39	1061	9.9	2.8	9.1
OsloCTM2	0.30	0.47	1557	1.2	19.5	41.0	OsloCTM2	1.27	1.95	1544	9.2	15.4	33.0
SPRINTARS	0.23	0.38	1658	1.1	27.9	58.7	SPRINTARS	1.33	1.66	1248	8.3	10.2	28.3
CAM4-Oslo-P1	0.36	0.52	1425	1.6	16.5	38.5	CAM4-Oslo-P1	0.67	0.89	1336	5.0	10.5	27.4
IMPACT-P1	0.50	0.54	1081	1.9	8.5	24.9	IMPACT-P1	0.96	0.87	904	5.4	5.6	19.8
OsloCTM2-P1	0.38	0.45	1189	1.7	5.9	16.0	OsloCTM2-P1	0.84	1.00	1189	6.8	6.6	18.1
Mean	0.37	0.51	1390	1.5	16.0	36.2	Mean	1.11	1.42	1259	f7.6	10.1	26.0
Std.dev	0.12	0.21	301	0.3	9.4	15.3	Std.dev	0.38	0.63	200	1.8	5.3	11.0

ACPD
12, 28929–28953, 2012

Black carbon vertical profiles strongly affect

B. H. Samset et al.

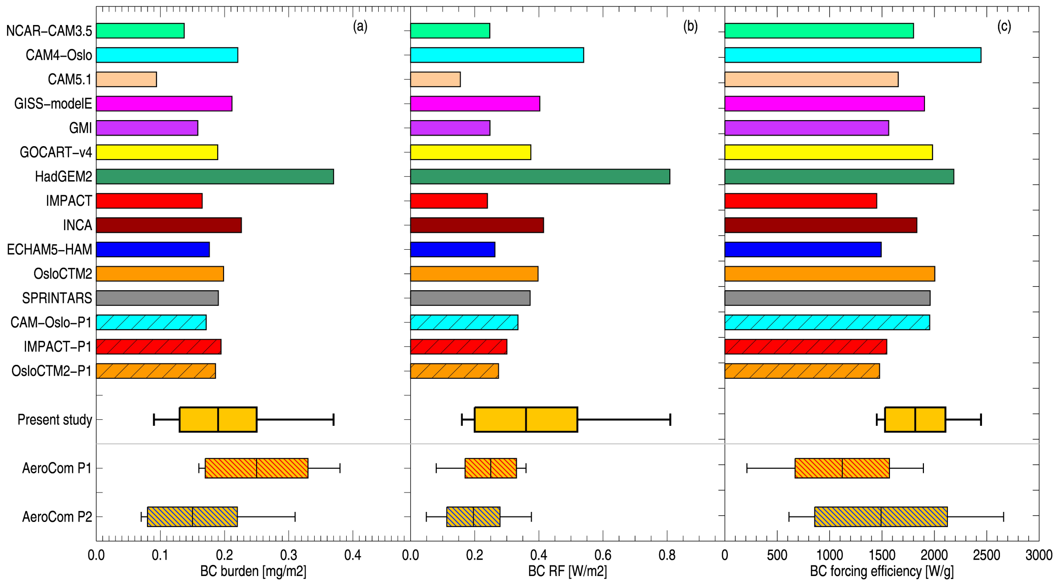

Fig. 1. Modeled BC global mean **(a)** burden, **(b)** RF and **(c)** forcing efficiency. Yellow boxes indicate mean, one standard deviation and max/min values. Mean values and spreads for AeroCom P1 and P2 (hatched whisker boxes) are taken from (Schulz et al., 2006) and (Myhre et al., 2012) respectively.

ACPD
12, 28929–28953, 2012

Black carbon vertical profiles strongly affect

B. H. Samset et al.

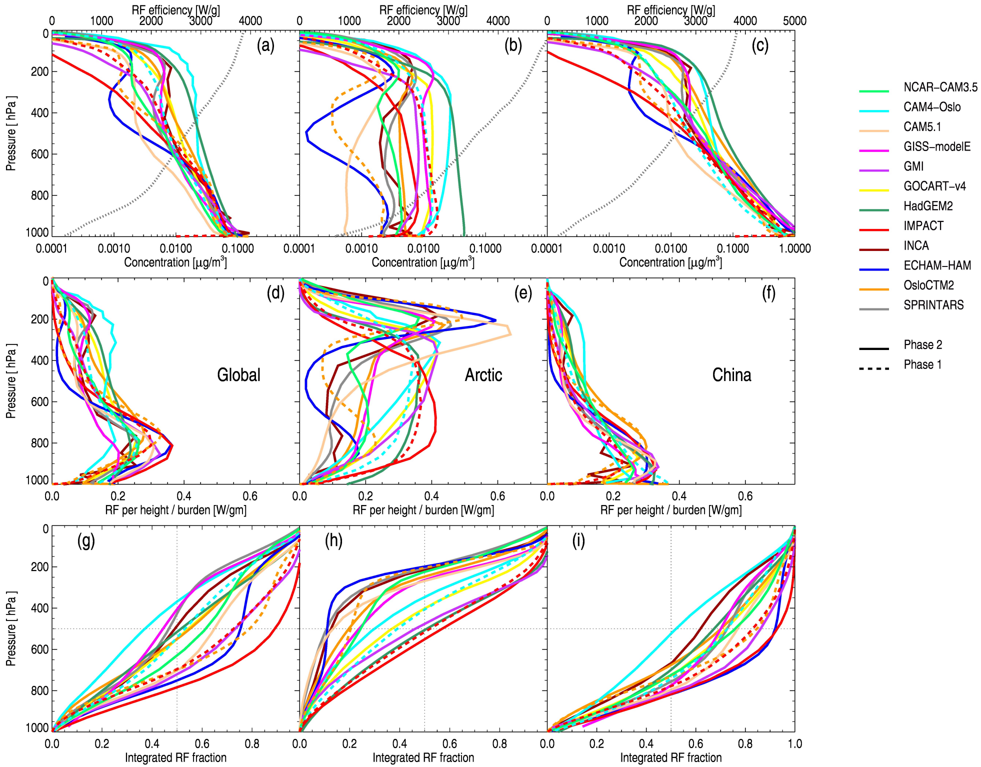

Fig. 2. Comparison of modeled concentration and RF profiles. **(a–c)** BC concentration vertical profiles, global mean and for two selected regions. Overlain is the annual mean forcing efficiency profile for the selected region (grey dashed line). Solid lines show AeroCom P2 submissions, dashed lines show P1. **(d–f)** BC RF per height, divided by the modeled global mean BC burden, globally and for three selected regions. **(g–i)** Vertical profile of integrated absolute BC RF. Lines indicate the 50 % mark and 500 hPa altitude.

ACPD
12, 28929–28953, 2012

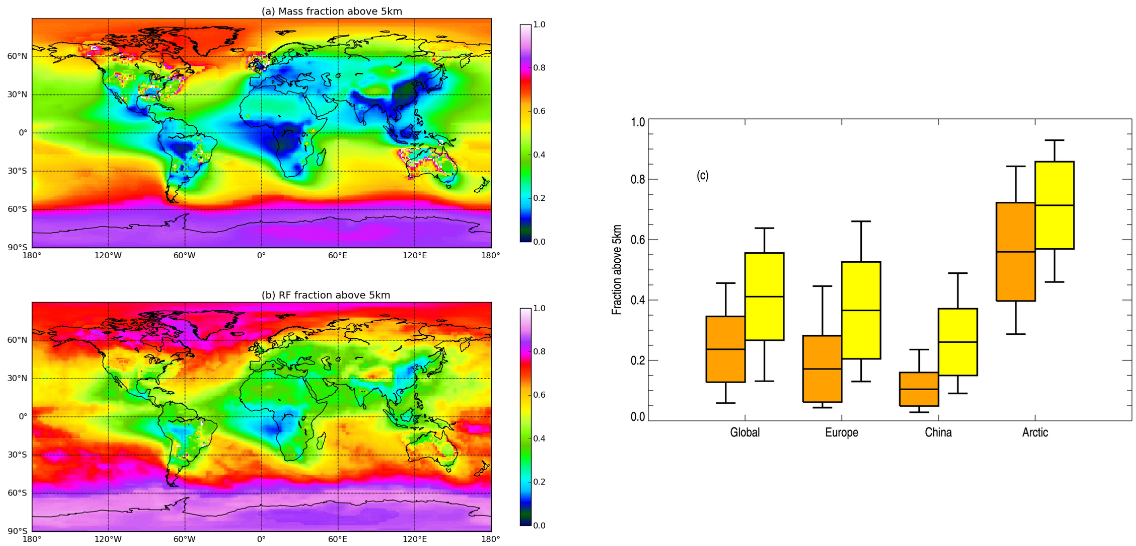

Fig. 3. Black carbon mass and induced forcing at high altitudes. **(a)** Fraction of modeled BC mass above 5 km. **(b)** Fraction of modeled BC RF originating above 5 km. **(c)** Mean fraction of mass (orange) and RF (yellow) globally and for three selected regions. Boxes indicate one standard deviation on the model spread, whiskers show maximum and minimum values.

ACPD
12, 28929–28953, 2012

Title Page
Abstract | Introduction
Conclusions | References
Tables | Figures
◀| |▶
◀ ▶
Back | Close
Full Screen / Esc
Printer-friendly Version
Interactive Discussion

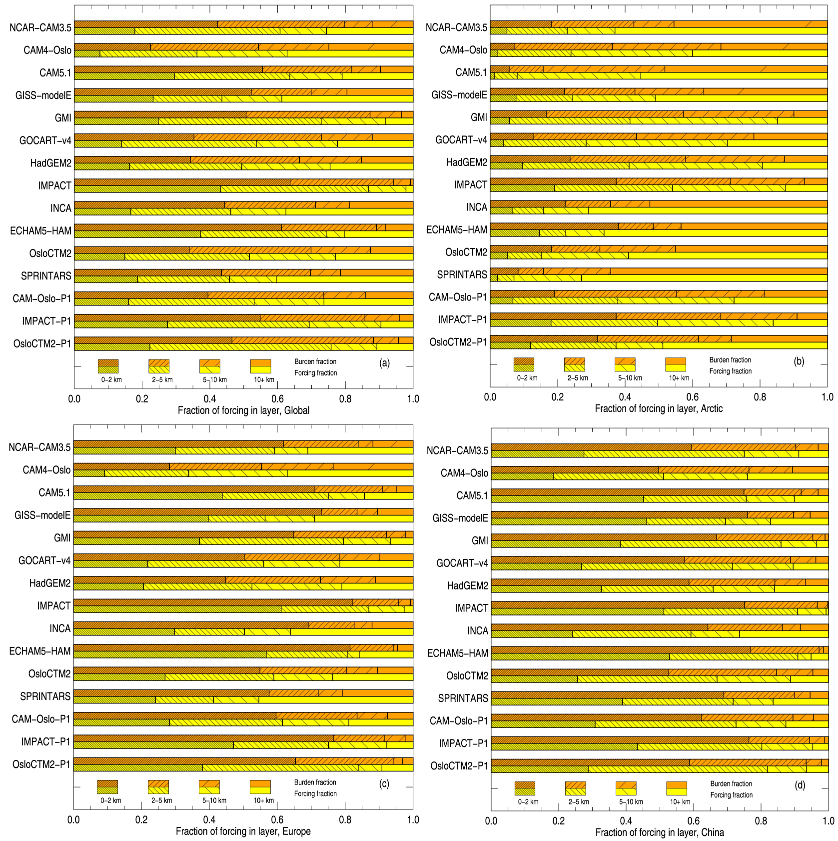

Fig. 4. Mass and forcing fractions in four altitude bands, globally and for three regions. Yellow boxes show mass fractions, orange boxes show RF fractions. **(a)** Global mean, **(b)** Arctic, **(c)** Europe, **(d)** China.

ACPD
12, 28929–28953, 2012

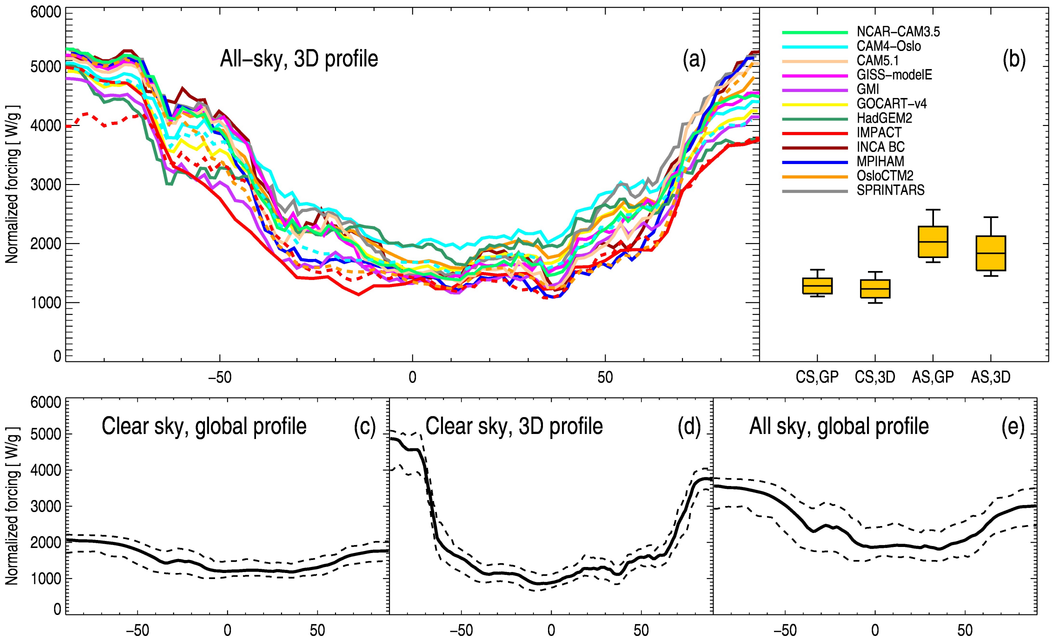

Fig. 5. Breakdown of spread in BC forcing efficiency. **(a)** Zonal mean of BC RF per gram using 3-D efficiency profiles and all sky conditions, for all models. **(c–e)** Model mean (solid line) and maximum/minimum (dashed lines) when instead using **(c)** a global, annual mean efficiency profile and clear sky conditions, **(d)** 3-D profile and clear sky conditions, and **(e)** a global profile and all sky conditions. **(b)** shows the global mean values for the four cases. Boxes show one standard deviation on the model spread, whiskers show maximum/minimum values.

ACPD
12, 28929–28953, 2012